HHS Public Access

Author manuscript

Mucosal Immunol. Author manuscript; available in PMC 2016 November 14.

Published in final edited form as:

Mucosal Immunol. 2016 September ; 9(5): 1278–1287. doi:10.1038/mi.2015.129.

Aspirin-triggered resolvin D1 is produced during self-resolving gram-negative bacterial pneumonia and regulates host immune responses for the resolution of lung inflammation

Raja Elie E. Abdulnour[a], **Ho Pan Sham**[a], **David N. Douda**[a], **Romain A. Colas**[b], **Jesmond Dalli**[b], **Yan Bai**[a], **Xingbin Ai**[a], **Charles N. Serhan**[b], and **Bruce D. Levy**[a,b]

[a]Pulmonary and Critical Care Medicine, Brigham and Women's Hospital and Harvard Medical School, Boston, MA, 02115, USA

[b]Center for Experimental Therapeutics and Reperfusion Injury, Department of Anesthesiology, Perioperative and Pain Medicine, Brigham and Women's Hospital and Harvard Medical School, Boston, MA, 02115, USA

Abstract

Bacterial pneumonia is a leading cause of morbidity and mortality worldwide. Host responses to contain infection and mitigate pathogen-mediated lung inflammation are critical for pneumonia resolution. Aspirin-triggered resolvin D1 (AT-RvD1; 7*S*,8*R*,17*R* trihydroxy-4Z,9E,11E,13Z,15E, 19Z docosahexaenoic acid) is a lipid mediator that displays organ protective actions in sterile lung inflammation, and regulates pathogen-initiated cellular responses. Here, in a self-resolving murine model of *Escherichia coli* pneumonia, lipid mediator metabololipidomics performed on lungs obtained at baseline, 24 hours and 72 hours after infection uncovered temporal regulation of endogenous AT-RvD1 production. Early treatment with exogenous AT-RvD1 (1 hr post-infection) enhanced clearance of *E.coli* and *Pseudomonas aeruginosa in vivo*, and lung macrophage phagocytosis of fluorescent *bacterial* particles *ex vivo*. Characterization of macrophage subsets in the alveolar compartment during pneumonia identified efferocytosis by infiltrating macrophages

Corresponding author: Prof. Bruce D. Levy, M.D., 77 Avenue Louis Pasteur, Boston, MA, 02115, Office phone: 617 525 5407, Office fax: 617 525 5413, blevy@partners.org.

Author contribution:

R.E.A contributed to experimental design, carried out experiments and data analyses and wrote the manuscript; H.P.S. and D.N.D. contributed to experimental design, carried out experiments and data analysis and contributed to manuscript and figure preparation; R.C. and J.D. carried out lipid mediator metabololipidomics and data analysis; C.N.S. contributed to experimental design, data analysis, and manuscript preparation; B.D.L contributed to experimental design, carried out experiments and data analyses, contributed to manuscript preparation, and conceived the overall research plan.

All authors concur with the submission and none of the data has been previously reported or is under consideration for publication elsewhere.

Competing financial interests declaration:

C.N.S. is an inventor on patents [resolvins] assigned to BWH and licensed to Resolvyx Pharmaceuticals. C.N.S. was scientific founder of Resolvyx Pharmaceuticals and owns founder stock in the company. C.N.S.' interests were reviewed and are managed by the Brigham and Women's Hospital and Partners HealthCare in accordance with their conflict of interest policies.

B.D.L. is an inventor on patents [resolvins] assigned to BWH and licensed to Resolvyx Pharmaceuticals. B.D.L.'s interests were reviewed and are managed by the Brigham and Women's Hospital and Partners HealthCare in accordance with their conflict of interest policies. The remaining authors declare that they have no competing interests or other interests that might be perceived to influence the results and/or discussion reported in this manuscript.

(CD11b^{Hi} CD11c^{Low}) and exudative macrophages (CD11b^{Hi} CD11c^{Hi}). AT-RvD1 increased efferocytosis by these cells *ex vivo*, and accelerated neutrophil clearance during pneumonia *in vivo*. These anti-bacterial and pro-resolving actions of AT-RvD1 were additive to antibiotic therapy. Taken together, these findings suggest that the pro-resolving actions of AT-RvD1 during pneumonia represent a novel host-directed therapeutic strategy to complement the current antibiotic centered approach to combatting infections.

Keywords

Resolution; pneumonia; macrophage; lipid mediator; AT-RvD1

Introduction

One critical function of the acute inflammatory host response to infection is delivery of leukocytes to sites of tissue injury to protect the host from microbial invasion and restore homeostasis[1]. If unrestrained in both amplitude and duration, persistent lung and airway infiltration by neutrophils can result in collateral injury to healthy bystander tissue, leading to organ damage and loss of function[2]. In health, inflammatory responses are self-limited with essential fatty acid derived specialized pro-resolving mediator (SPM) signaling pivotal to the arrest of inflammation and initiation of resolution[1]. Aspirin-triggered resolvin D1 (AT-RvD1; 7S,8R,17R trihydroxy-4Z,9E,11E,13Z,15E,19Z docosahexaenoic acid) was first identified as a product of aspirin acetylated cyclooxygenase-2[3, 4]. It is now clear that AT-RvD1 is a docosahexaenoic acid (DHA) derived SPM that can also be produced endogenously in the absence of aspirin by a second pathway initiated by cytochrome P450 enzymes[5]. AT-RvD1 potently decreases acute lung inflammation after mucosal injury[6]; however, its role in pneumonia remains to be characterized.

Bacterial pneumonia is a leading cause of mortality and morbidity worldwide, accounting for over 110 million years of life lost in 2010[7]. Gram-negative bacterial pneumonia is the most common life-threatening hospital acquired infection[8]. In the United States, pneumonia causes more disease and death than any other infection, and there has been little change in pneumonia-associated mortality for more than five decades[9]. Currently, antibiotics are the cornerstone of therapy; however, the rise of antibiotic-resistant microorganisms emphasizes a need for a new approach that augments host defense mechanisms to microbial invasion[10]. Stimulation of bacterial clearance and counter regulation of inflammatory responses are defining features of SPMs[11]. Given its potent actions in regulating sterile lung inflammation[6], and pathogen-initiated cellular responses *in vitro*[12], we hypothesized that the SPM AT-RvD1 would be produced during pneumonia to limit infection and ensuing inflammatory responses.

Alveolar macrophages are tissue resident cells with key functions in pathogen recognition, initiation of host defense via protective inflammation, and in clearance of invading microbes[11]. Additional macrophage subsets infiltrate the alveolar space during the course of pathogen-mediated acute lung inflammation[13] to augment the resident macrophage protective actions[14]. Of interest, macrophages carry the biosynthetic and molecular circuitry

to produce and respond to SPM[1]. Here, in a self-resolving murine model of *Escherichia coli* (*E. coli*) pneumonia, AT-RvD1 was produced in a temporally regulated and enhanced gram-negative bacterial clearance and resolution of pathogen-initiated lung inflammation.

Materials and methods

Materials

AT-RvD1 (7*S*,8*R*,17*R*-trihydroxy-4Z,9E,11E,13Z,15E,19Z-docosahexaenoic acid) was obtained from Cayman Chemical (Ann Arbor, MI, USA) and validated just prior to use with LC-MS-MS and physical criteria reported earlier[15]. *E. coli* (O6:K2:H1) strain ATCC 19138 and *Pseudomonas aeruginosa* (*P. aeruginosa;* HER-1018) strain ATCC BAA-47 were obtained from the American Type Culture Collection (Manassas, VA, USA). *E. coli* particles conjugated with pHrodo were purchased from Life Technologies (Carlsbad, CA, USA). Lipopolysaccharide (LPS, *E. coli* O55:B5), ciprofloxacin, and hydrochloric acid (HCl) were purchased from Sigma-Aldrich (St. Louis, MO, USA). FACS antibodies were obtained from eBioscience (San Diego, CA, USA): F4/80 (BM8); Biolegend (San Diego, CA, USA): CD11b (M1/70), and Ly6G (1A8); BD Biosciences (San Diego, CA, USA): CD11c (HL3), CD45 (30-F11). Permeabilization buffer was purchased from eBioscience.

Mice

C57BL/6 male mice (8–10 wk old, body weights 20–25 g; Charles River Laboratories, Wilmington, MA, USA) were housed in isolation cages in pathogen-free conditions on a light–dark cycle with light from 7:00 to 20:00 at 25°C. Mice were fed a standard diet (Laboratory Rodent Diet 5001; PMI Nutrition International, St. Louis, MO, USA) containing 4.5% total fat with 0.3% ω-3 fatty acids and <0.02% C20:4 and were provided water ad libitum. All studies were reviewed and approved by the Harvard Medical Area standing committee on animals.

Murine model of gram-negative bacterial pneumonia

Live *gram-negative bacteria* (*E. coli* or *P. aeruginosa*, 1×10^6 CFU in 25 μl saline) were instilled selectively into the left mainstem bronchus of anesthetized mice (C57bl/6, male, 8–10 weeks; Charles River) as in[16]. Mice received AT-RvD1 (100 ng, IV) or vehicle (<0.1% (vol/vol) ethanol in saline) 1 hr after intra-bronchial *E. coli* or *P. aeruginosa*. In select experiments, mice received ciprofloxacin (0.2, 2, or 20 mg/kg, IP) or vehicle in addition to AT-RvD1, 1 hr after intra-bronchial *E. coli*. In separate experiments, animals were treated with AT-RvD1 (100 ng, IB) or vehicle via a repeat tracheostomy surgery 24 and 36 hrs after high-dose intra-bronchial *E. coli* (2×10^6 CFU). A high dose of *E. coli* was used to induce neutrophil infiltration comparable to LPS-induced lung inflammation. In pathogen-mediated acute lung inflammation experiments, animals were treated with *E. coli* LPS (0.3 mg/kg, 50 μl in saline, IB). In sterile acute lung inflammation experiments, hydrochloric acid (HCl, 0.1N, pH ~1.0, 50 μl IB) was administered as in[17].

Bacterial CFU determination

At select time-points after intra-bronchial bacteria (*E. coli* or *P. aeruginosa*), lungs were collected aseptically and homogenized in 2.5 ml of ice-cold sterile saline. Aliquots of serial

dilutions were plated LB-agar plates. After incubation for 24 hrs at 37°C, colonies were counted and results were expressed as CFU per whole lungs.

Lipid mediator metabololipidomics

Lung tissue isolates were disrupted gently in methanol then processed for LC-MS-MS as in[17]. AT-RvD1 levels were monitored and quantified with multiple reaction monitoring (MRM) developed using signature ion fragments for AT-RvD1 (m/z = 375/141) and d_5-RvD_2 (m/z = 380/141)[15]. Quantification was carried out on the basis of the peak areas obtained with MRM transitions and linear calibration curves for synthetic mediators, and deuterated standards for recoveries[15].

Bronchoalveolar lavage

At timed intervals, mice were euthanized and the trachea exposed. A 20-gauge angiocatheter was inserted into the trachea and the lungs were lavaged with two separate 1 ml volumes of ice-cold PBS with 0.6 mM EDTA. The bronchoalveolar lavage (BAL) fluid was pooled, centrifuged at 500 × g for 5 minutes at 4°C to pellet the cell fraction. The cell pellet was resuspended in cold PBS.

FACS analysis and cell sorting

BAL cells were obtained after centrifugation of pooled BAL fluid, and the cell pellet was stained with fluorochrome-labelled antibodies to obtain a leukocyte differential; neutrophils ($CD45^+$ $F4/80^-$ $Ly6G^+$ $CD11b^+$), infiltrating macrophages (iMacs; $CD45^+$ SSc^{High} $F4/80^+$ $CD11c^{Low}$ $CD11b^+$), exudative macrophages (ExMacs; $CD45^+$ SSc^{High} $F4/80^+$ $CD11c^{High}$ $CD11b^+$), and resident alveolar macrophages (rAM; $CD45^+$ $F4/80^+$ SSc^{High} $CD11c^{High}$ $CD11b^-$). Cell counts were obtained by adding a known amount of fluorescent counting beads (CountBright, Life Technologies) to the BAL cell pellet prior to flow cytometry as per the manufacturer's recommendations, and normalized to lavage. FACSCanto II (BD Biosciences) and FlowJo Ver. 10 software (Tree Star, Ashland, OR, USA) were used for analyses. In some experiments, five BALFs were pooled and F4/80 positive macrophage subsets cells were sorted with > 95% purity, using FACSaria (Beckton-Dickinson). The sorted populations were used for *ex vivo* efferocytosis assays. For sorting of macrophage subsets, BALF obtained 72 hrs after intra-bronchial LPS was used, as LPS resulted in the highest maximal number of macrophages (see Results) allowing for a better yield of each macrophage subset using fluorescence activated cell sorting.

Determination of bioactive molecule levels in BALF

Select cytokines were measured in aliquots of pooled BALF using a bead-based immunoassay as per the manufacturer's instructions (LEGENDPlex by Biolegend, San Diego, CA, USA). Lipocalin 2 levels in BAL fluid were determined by enzyme-linked immunosorbent assay (Lipocalin 2 Quantikine ELISA Kit, R&D Systems, Minneapolis, MN, USA). LPS levels in BAL fluid were determined using a *Limulus* Amebocyte Lysate endotoxin quantitation kit (ThermoFisher Scientific, Cambridge, MA). All measurements were normalized to volume of pooled BAL fluid.

Ultra-thin lung sections

Lung sections were prepared as described previously[18]. Briefly, after euthanasia of naïve animals by isoflurane overdose, the lungs were exposed and slowly perfused free of blood with 5 ml HBSS. The lungs were then inflated with 1.2 ml agarose (low melting point, Life Technologies, NY) in HBSS (1.5%) via a tracheal catheter (model 20G Intima, Becton Dickinson). After the agarose solidified, one lung lobe was separated and sectioned into 150 um-thick slices using a tissue slicer (VF-300; Precisionary Instruments, Greenville, NC). Lung slices were incubated at 5% CO2, 37C in DMEM/F-12 supplemented with penicillin-streptomycin (Invitrogen, Cambridge, MA) overnight.

Phagocytosis assay

Ultra-thin lung sections were washed in HBSS then stained with anti-CD11c (FITC) and treated with AT-RvD1 (10 nM) for 30 minutes at 37°C. The lung sections were then washed before addition of *E. coli* particles conjugated to pHrodo red dye (100 μg/ml, Life Technologies, NY). To maximize the sensitivity in detecting an increase in phagocytosis, a dose-response curve of *E. coli* particles per lung section was performed to have as little phagocytosis as possible by untreated lung sections. Sections were observed with Nikon Eclipse TS 100 epi-fluorescence microscopy with filter sets for indicator dye of Phrodo Red (green excitation) or FITC (blue excitation) at 0 and 60 minutes after addition of the *E. coli* particles. Images were then overlayed, and $CD11c^+$ cells were enumerated. Phagocytosis was quantified as the ration of $CD11c^+$ $E. coli^+$ cells over $CD11c^+$ cells.

Macrophage efferocytosis

Macrophage efferocytosis was quantified as previously described[19]. Briefly, neutrophils were obtained from peritoneal lavage fluid obtained 4 hrs after zymosan A (1 mg, IP) – induced murine peritonitis, and labeled with carboxyfluorescein diacetate-succinimidyl ester (CFDA; 10μM, 30 min, 37°C) and cultured overnight (serum free media) to induce apoptosis (confirmed by >95% Annexin V+ 7AAD- surface expression by flow cytometry, data not shown). Murine alveolar macrophage subsets were sorted from BALF obtained 72 hrs after IT LPS according to the gating strategy detailed above and allowed to adhere in a 96-well plate for one hour at a density of 2.5×10^4 cells/well. The macrophages were then incubated with AT-RvD1 for 30 minutes at 37°C before the addition of apoptotic neutrophils (1.25×10^5 cells/well, macrophage to neutrophil ratio of 1:5). After 60 minutes of co-incubation, trypan blue (1:2) was added to quench CFDA in extracellular neutrophils, and the number of phagocytosed cells (i.e., intracellular) was determined using a FLX-800 (Biotek, Inc) plate reader (Molecular Devices) by monitoring fluorescence emission at 525 nm.

Histopathology and immunohistochemistry

Lung tissue was fixed by inflation with Zinc Fixative (BD Pharmingen, San Diego, CA, USA) at a transpulmonary pressure of 20 cm H_2O and embedded in paraffin. For histological analysis, lungs were collected 0, 24, and 48 hrs after *E. coli* instillation and paraffin-embedded 5-μm sections of lungs were cut and stained with H&E for light microscopy. In order to detect bacteria, *E. coli* staining was performed using an anti-*E. coli* antibody (GeneTex, CA) and an anti-rabbit secondary antibody (Abcam, MA). Leica

DFC480 and Leica QWin Standard V3.4.0 (Leiica Microsystems Ltd) were used for microscopic analysis.

Statistical analysis

All data are expressed as means ± SD. Comparisons between groups were conducted using ANOVA and Student's t test as appropriate. A level of $p \leq 0.05$ was considered to indicate statistical significance. Statistics were performed using Graphpad Prism 6.0 for Windows (San Diego, CA). For multivariate statistical analysis, principal component analysis (PCA) was performed using SIMCA 13.0.3 software (Umetrics, Umea, Sweden) following mean centering and unit variance scaling of lipid mediator amounts as in[15]. The score plot shows the systematic clusters among the observations (closer plots presenting higher similarity in the data matrix). Loading plots describe the magnitude and the manner (positive or negative correlation) in which the measured LM-SPM contribute the cluster separation in the score plot.

Results

Endogenous AT-RvD1 is produced during self-resolving *E. coli* pneumonia

To determine endogenous SPM production during lung infection, we used a self-resolving model of *E. coli* pneumonia. After intra-bronchial instillation of *E. coli* (see Methods), the resultant CFU at 6 hrs ($154.5\times10^3 \pm 26.4\times10^3$ CFU, mean ± SD) and 24 hrs ($3.0\times10^3 \pm 2.7\times10^3$, mean ± SD) were consistent with effective bacterial clearance (Figure 1a). Neutrophil counts peaked at 24 hrs ($450.3\times10^3 \pm 161.1\times10^3$ cells/BALF, mean ± SD) and returned to near baseline within 72 hrs ($15.2\times10^3 \pm 3.9\times10^3$ cells/BALF, mean ± SD) (Figure 1a). At 48 hrs post-infection, neutrophil counts were approximately half-maximal ($210.8\times10^3 \pm 84.4\times10^3$ cells/BALF, mean ± SD) and macrophage counts peaked ($353.5\times10^3 \pm 50.0\times10^3$ cells/BALF, mean ± SD). Within 72 hours, macrophage numbers also returned to near baseline ($124.4\times10^3 \pm 40.3\times10^3$ cells/BALF, mean ± SD) (Figure 1a). *E. coli* was not detected in murine peripheral blood (data not shown). Murine lungs were obtained 0, 24, and 72 hrs after *E. coli* infection and SPM were extracted from lung homogenates for lipid mediator (LM) metabololipidomic analysis (see Methods). In this murine model of bacterial pneumonia, LM metabololipidomic profiling of lung tissue revealed temporal regulation of SPM production with several mediators increasing after infection (Table 1). Each of the mediators was identified in accordance with established criteria, including LC retention time and diagnostic ions in MS/MS. A principal component analysis (PCA, see Methods and reference[15]) gave distinct clustering for lipid mediator profiles obtained from 24 hrs and 72h hrs (Figure 1b–c). The loading plot demonstrated that SPM levels were selectively regulated and associated with the resolution phase (i.e., 72 hours) (Figure 1c). Of note, AT-RvD1 showed tight clustering among samples, as indicated by little deviation along principal component 2 (Figure 1c). After *E. coli* infection, lung AT-RvD1 was determined by LC-MS/MS criteria (Figures 1d–e) and progressively increased at 24 and 72 hrs (~11.2 fold increase 72 vs 0 hrs) (Figure 1f and Table 1).

AT-RvD1 enhances gram-negative bacterial clearance after lung infection

Temporal regulation of endogenous AT-RvD1 during pneumonia suggested it might exert host protective mechanisms during lung infection, so we next investigated its actions on bacterial clearance *in vivo*. Treatment of animals with AT-RvD1 (100 ng IV, ~ 4 μg/kg) one hour after infection led to a marked decrease in lung *E. coli* compared to untreated animals (Figures 2a, S1a) and significant reductions in lung bacterial burden at 6 hrs (25.6% decrease, Figure 2b) and 24 hrs (90.3% decrease, Figure 2c) after infection. The increased clearance of *E. coli* was associated with increased physical activity in AT-RvD1 treated animals as early as 6 hours after infection (see Supplementary Movie 1 in the online supplement). AT-RvD1 had no direct antimicrobial activity on bacterial cultures (data not shown). Of interest, AT-RvD1 also selectively regulated BALF cytokine levels with significant decreases in IL-6 (Figure 2d) and TNFα (Figure 2e). Levels of IL-1α, MCP-1, and IL-10 were not significantly changed by AT-RvD1 (Figure S1b). In addition to *E. coli* AT-RvD1 significantly increased lung *P. aeruginosa* bacterial clearance (61.6% decrease in CFU 6 hrs after infection, Figure 2f).

AT-RvD1 increases macrophage phagocytosis of *E. coli* particles *in situ*

To determine mechanisms for AT-RvD1's anti-microbial actions, we examined lung macrophage-mediated killing. To this end, fresh ultra-thin sections of perfused lungs from naïve mice were stained with a fluorochrome labeled anti-CD11c antibody and treated with AT-RvD1 or vehicle. These lung slices from naive animals have preserved airway and alveolar architecture and tissue resident cells, including macrophages. No granulocytes were present (see Methods). *E. coli* particles conjugated with a pH-sensitive reporter were incubated with the lung sections for 60 min. The reporter is designed to indicate engulfment of the *E. coli* particles into acidic phagolysosomes[20]. A dilute concentration of particles was used to minimize background phagocytosis of *E. coli* particles during this time interval in vehicle exposed control lung sections (Figures 3a and c). Incubation with AT-RvD1 (10 nM, 60 min) significantly increased phagocytosis by CD11c+ lung macrophages (Figures 3b and c).

AT-RvD1 increases levels of the anti-microbial peptide lipocalin 2

Since Aderem and colleagues found that the antimicrobial peptide lipocalin 2 plays important roles in host responses to *E. coli*[21]), we next determined the impact of AT-RvD1 on BAL fluid lipocalin 2 levels. Six hours after *E. coli* infection, lipocalin 2 was significantly increased (336.4 ng/ml ± 158.2, mean ± SD, $P \leq 0.05$) relative to uninfected mice (38.27 ng/ml ± 20.56, mean ± SD, Figure 3d). AT-RvD1 further increased BAL lipocalin 2 levels (553.0 ng/ml ± 346.6, $P \leq 0.05$, Figure 3d).

Macrophage subsets during self-resolving lung infection

Neutrophil clearance occurred concomitant with increased AT-RvD1 levels and lung macrophage numbers (Figure 1), suggesting regulation of macrophages by AT-RvD1 for resolution of pathogen-initiated lung inflammation. CD11b and CD11c surface expression by BALF macrophages after *E. coli* infection was determined using flow cytometry, leading to the identification of three lung macrophage subsets in the alveolar compartment (Figure

4a); infiltrating macrophages (iMacs, $CD11c^{Low}$ $CD11b^{+}$), exudate macrophages (ExMacs, $CD11c^{Hi}$ $CD11b^{+}$), and resident alveolar macrophages (rAM, $CD11c^{Hi}$ $CD11b^{-}$) (Figure 4b). The presence of iMacs and ExMacs was transient, peaking 48 hrs after infection (7.1×10^{3}±5.2 iMacs/BALF, 35.2±17.23 ExMacs/BALF at 48 hrs, mean±SD.), while rAM numbers did not significantly change (Figures 4c–d). iMacs and ExMacs were also identified in self-resolving acid-induced sterile lung injury (Figure S2a), and LPS-induced lung inflammation (Figure S2b). Intra-bronchial LPS resulted in a higher maximal number of macrophages compared to *E. coli* infection and HCl-induced lung injury (Figure S2c). Specific intracellular Ly6G immunostaining of BALF macrophages obtained 48 hrs after *E. coli* infection (Figures 5a–b), and 72 hrs after intra-bronchial LPS (Figures S3a–b), showed a significant increase in Ly6G+ iMacs and ExMacs, but not in rAM.

AT-RvD1 promotes efferocytosis by macrophages

To determine if AT-RvD1 regulates this pro-resolving macrophage action[11], macrophage subsets were sorted from BALF obtained 72 hrs after LPS, exposed to AT-RvD1 (10 nM, 30 min, 37°C) then incubated with fluorescent apoptotic neutrophils for 1 hr. Phagocytosis of apoptotic neutrophils was then determined by measuring intracellular macrophage fluorescence (see Methods). AT-RvD1 significantly increased efferocytosis by iMacs, and to a lesser extent by ExMacs (Figure 5c). We next examined the impact of AT-RvD1 on neutrophil clearance *in vivo*. Animals were treated with AT-RvD1 (100 ng, IB) for increased alveolar delivery to macrophages. When given at 24 hrs and 36 hrs, AT-RvD1 (IB) significantly decreased BAL neutrophils after *E. coli* (25.0%, Figure 5d) and in separate experiments after LPS (38.1%, Figure S3c). Collectively, these findings demonstrate that AT-RvD1 promotes clearance of apoptotic neutrophils by macrophage subsets and accelerates alveolar neutrophil clearance for resolution of pathogen-mediated lung inflammation.

AT-RvD1 enhances bacterial clearance in combination with antibiotics

To determine if AT-RvD1 actions on host responses to *E. coli* infection provide additional benefit to antibiotics, mice were treated 1 hr after *E. coli* with AT-RvD1 (100 ng, IV), ciprofloxacin at its IC_{50} dose for *E. coli* (0.2 mg/kg, IP) (Figure S4a), or both AT-RvD1 and ciprofloxacin (see Methods). Lung CFUs were significantly decreased in mice treated with AT-RvD1 (24.9% reduction compared to untreated mice) (Figure 6a). In addition, mice that received both AT-RvD1 and ciprofloxacin had significantly less CFU than mice treated with antibiotics alone (Figure 6a). Of note, AT-RvD1 significantly decreased BAL fluid LPS (2.7±0.7 EU/ml BAL fluid, mean ± SD, $P \leq 0.05$) compared to untreated animals (5.5±0.7 EU/ml BAL fluid, mean ± SD, Figure 6b). In sharp contrast, ciprofloxacin alone did not decrease BAL fluid LPS (5.6±0.7 EU/ml BAL fluid, mean ± SD) despite the decrease in CFU (Figures 6a–b). In combination with ciprofloxacin, AT-RvD1 decreased the LPS levels (4.1±0.6 EU/ml BAL fluid, mean ± SD, $P \leq 0.05$, Figure 6B). Moreover, AT-RvD1 treatment significantly decreased BALF neutrophils 48 hrs after infection (55.0% reduction in BALF neutrophil counts compared to untreated animals, Figure 6b), whereas antibiotic therapy had no significant impact on BALF neutrophils (Figure 6b). Combined AT-RvD1 and antibiotic treatment was additive and resulted in the lowest BALF neutrophil count (70% reduction in BALF neutrophil count compared to untreated animals, Figure 6b). At 48 hrs post-infection,

BALF neutrophil numbers were half-maximal and declining with macrophages rising to roughly equal numbers (Figure 1a). As an index to tissue resolution, the BALF macrophage to neutrophil ratio was 1.3 in vehicle control mice and increased to 1.7 with AT-RvD1 ($P=0.06$, Figure 6c). Ciprofloxacin alone did not significantly impact the macrophage to neutrophil ratio (1.2); however, the ratio was significantly increased to 2.6 by combination of ciprofloxacin and AT-RvD1 ($P<0.05$, Figure 6c). Histological examination of animals at this time point after infection revealed decreased cellularity and alveolar wall edema in animals treated with AT-RvD1 compared to vehicle exposed animals and animals treated with ciprofloxacin alone (Figure 6d). Collectively, these results indicate that AT-RvD1 enhanced antibiotic-mediated bacterial clearance, and decreased pathogen-initiated lung inflammation.

Discussion

Bacterial clearance and counter-regulation of pathogen-mediated inflammation define resolution of bacterial pneumonia[9]. While antibiotics are crucial for the former, they have little impact on clearance of inflamed tissue. Results presented herein demonstrate that endogenous AT-RvD1 levels increased during self-resolving *E. coli* pneumonia, suggesting a role for AT-RvD1 during lung catabasis. Exogenous AT-RvD1 treatment enhanced clearance of two gram-negative bacteria *in vivo*, in part via increased bacterial particle phagocytosis by resident macrophages and increased tissue levels of the anti-microbial peptide lipocalin 2. In addition, AT-RvD1 engaged macrophage subsets for phagocytosis of apoptotic neutrophils, increased alveolar neutrophil clearance, and decreased alveolar LPS levels. When combined with antibiotic therapy, AT-RvD1 further enhanced bacterial clearance, mitigated antibiotic-mediated LPS release, and promoted resolution of *E. coli*-initiated lung inflammation.

Lipid mediator metabololipidomics profiling of the resolving exudates allows for sensitive detection of endogenous SPM production[1]. In the present work, metabololipidomic profiling identified temporal and selective regulation of SPM during bacterial pneumonia. Levels of several SPM were increased during the resolution phase (from 24 to 72 hrs after infection, Figure 1a), likely a result of increased precursor availability in the resolving exudate[22, 23], and biosynthetic enzyme activation[24]. Principal component analysis identified several SPM that contributed to time-point separation, in particular AT-RvD1. Biosynthesis of AT-RvD1 in the absence of aspirin exposure is likely initiated via oxygenation at the carbon-17 position of DHA by cytochrome p450 enzymes[5], which are abundant in the lungs[25]. Indeed, animals deficient in CYP1 monooxygenases demonstrate decreased levels of 17-hydroxy-DHA[26]. Increased resistance to metabolic inactivation of AT-RvD1 relative to its 17 carbon position epimer RvD1 may account for its more consistent levels in the PCA loading plot and a pharmacological advantage for pneumonia[4].

Resolution of lung mucosal inflammation is a defining characteristic of SPM[27]. Eicosapentaenoic acid-derived resolvin E1 (RvE1) promotes the resolution of allergic airway inflammation[28], arachidonic acid-derived 15-epi-lipoxin A_4 enhances resolution of acute lung injury[29], and DHA-derived maresin 1 protects lung function during acid-induced lung injury[17]. AT-RvD1 decreases nuclear factor-kB signaling for organ protection after sterile acute lung inflammation[6], and attenuates pro-inflammatory signaling in human airway epithelial cells[30]. These anti-inflammatory and pro-resolving actions are not

immune-suppressive during bacterial infection[11]. Indeed, select DHA-derived resolvins and their counter-regulatory circuits enhance bacterial clearance by leukocytes[31], and protect from polymicrobial murine sepsis[3132]. In the lung, RvE1 treatment attenuates mucosal injury and protects animals from aspiration pneumonia[16]. Results presented herein uncover direct AT-RvD1 actions on host-mediated anti-bacterial responses, and concomitant pro-resolving actions, emphasizing that SPMs are leads for multi-pronged therapy against bacterial pneumonia. Mechanisms for enhancing bacterial clearance include stimulating leukocyte phagocytosis of the offending agent[11]. In allergic airway inflammation, AT-RvD1 increases macrophage phagocytosis of antigen-coated particles[33], and RvD1 increases neutrophil phagocytosis of bacteria during extra-pulmonary infection[34]. Our results demonstrated an increase in macrophage phagocytosis of bacterial particles in live lung tissue. In addition to enhancing phagocyte function, AT-RvD1 increased levels of the antimicrobial peptide lipocalin 2 to provide an additional mechanism for mucosal host defense. Of note, metabololipidomic profiling of infected lungs demonstrated regulation of additional SPMs. Their contribution to host protection during pneumonia is under investigation.

In addition to their defensive role against bacterial invasion, macrophages are crucial effectors of resolution of inflammation[1]. Examination of peritoneal macrophages during peritonitis identified a subset of macrophages with a M2 signature present only during resolution[35], and a subset of CD11b^{Lo} macrophages that emigrate to nearby lymphoid organs for termination of inflammation[36]. Both peritoneal macrophage subtypes had decreased phagocytic ability. In the lung, macrophage phenotyping during resolving inflammation has identified two distinct subsets in addition to rAM[13, 14]. Their activation markers are intermediate between M1 and M2, and both demonstrate increased CD11b expression. Findings presented here indicate that these macrophage subsets appear during resolution of pathogen-initiated lung inflammation and efferocytose apoptotic neutrophils. As such, iMacs and ExMacs are distinct from resolving macrophages identified during peritoneal inflammation. In our model of pathogen-initiated lung inflammation, their time course positions them for roles in the resolution of inflammation, as they infiltrate into the alveolar space during neutrophil clearance. Towards this end, ExMacs release IL1ra for organ protection during bacterial pneumonia[14]. In addition, results presented here demonstrate efferocytosis of apoptotic neutrophils by iMacs and ExMacs. Furthermore, AT-RvD1 regulation of iMacs and ExMacs efferocytosis of apoptotic neutrophils uncovered a role for these macrophages as SPM cellular targets to promote pneumonia resolution. Of note, the analyses here were focused on BALF macrophages; however, myeloid-derived suppressor cell -like cells are in lung interstitium after bacterial pneumonia and also participate in tissue resolution by efferocytosis[37].

Pneumonia continues to have a substantial impact on the global burden of disease with elevated mortality[7], and increasing prevalence of antibiotic-resistant bacteria[38], in particular gram-negative bacteria in nosocomial infections[8]. Therapies targeting host-responses to infection offer the possibility of augmenting antibiotics to improve outcomes[9]. Anti-inflammatory therapies, such as corticosteroids, have not proven successful[39], likely secondary to concomitant immune suppression. In sharp contrast to immunosuppressive agents, SPM engage endogenous resolution pathways that enhance bacterial host defense.

Macrophages carry the dual effector functions of host defense and pro-resolution[11], thus represent ideal cell-based therapeutic targets. Results presented here show that antibiotic treatment alone had little effect on the resolution of lung inflammation, in part related to persistent increases in LPS likely induced by the bactericidal actions of ciprofloxacin[40]. AT-RvD1 significantly promoted resolution through macrophage activation for phagocytosis, decreased BAL fluid LPS, and increased BAL fluid lipocalin 2 (an important anti-microbial peptide for *E. coli* host defense[21]). In conjunction with AT-RvD1's protective actions on lung barrier integrity and mechanics[6], these new pro-resolving mechanisms in bacterial defense emphasize roles for SPM in promoting resolution of pathogen-initiated tissue inflammation[31, 34], and help further distinguish pro-resolution from anti-inflammation[11].

In summary, our findings have uncovered new roles for AT-RvD1 in promoting resolution of *gram-negative bacterial* pneumonia. In this study, the DHA-derived lipid mediator AT-RvD1 was endogenously produced in a temporally regulated manner, enhanced bacterial clearance by direct actions on lung macrophages and lipocalin 2, and promoted the resolution of inflammation by directly increasing efferocytosis of apoptotic neutrophils by macrophage subsets in the alveolar space. These actions augmented antimicrobial therapy, thus offering a potential new host-directed therapeutic approach to the global threat of bacterial pneumonia that emphasizes endogenous resolution signaling pathways.

Supplementary Material

Refer to Web version on PubMed Central for supplementary material.

Acknowledgments

We thank Hiroyuki Seki and Iliyan K. Vlassakov for technical assistance. This research was supported in part by the US National Institutes of Health T32-HL07633 (R.E.A., B.D.L.), R01-HL068669 (B.D.L.), and P01-GM095467 (B.D.L., C.N.S). The content is solely the responsibility of the authors and does not necessarily reflect the official views of NHLBI, NIGMS, or the National Institutes of Health.

Abbreviations

ARDS	acute respiratory distress syndrome
AT-RvD1	Aspirin-triggered resolvin D1 (7S,8R,17R-trihydroxy-docosa-4Z,9E,11E, 13Z,15E,19Z hexaenoic acid)
CFU	colony-forming units
E. coli	Escherichia coli
ExMacs	exudative macrophages
iMacs	infiltrating macrophages
IP	intra-peritoneal
IB	intra-bronchial
IV	intra-venous

LM	lipid mediator
RvD1	resolvin D1 (7S,8R,17S-trihydroxy-docosa-4Z,9E,11E,13Z,15E,19Z-hexaenoic acid)
SPM	specialized pro-resolving mediator
LPS	lipopolysaccharide

References

1. Serhan CN. Resolution phase of inflammation: novel endogenous anti-inflammatory and proresolving lipid mediators and pathways. Annual review of immunology. 2007; 25:101–137.
2. Matthay MA, Ware LB, Zimmerman GA. The acute respiratory distress syndrome. J Clin Invest. 2012; 122(8):2731–2740. [PubMed: 22850883]
3. Serhan CN, Hong S, Gronert K, Colgan SP, Devchand PR, Mirick G, et al. Resolvins: A Family of Bioactive Products of Omega-3 Fatty Acid Transformation Circuits Initiated by Aspirin-Treatment that Counter Proinflammation Signals. J Exp Med. 2002; 196(8):1025–1037. [PubMed: 12391014]
4. Sun YP, Oh SF, Uddin J, Yang R, Gotlinger K, Campbell E, et al. Resolvin D1 and its aspirin-triggered 17R epimer. Stereochemical assignments, anti-inflammatory properties, and enzymatic inactivation. J Biol Chem. 2007; 282(13):9323–9334. [PubMed: 17244615]
5. Serhan CN, Petasis NA. Resolvins and protectins in inflammation resolution. Chemical reviews. 2011; 111(10):5922–5943. [PubMed: 21766791]
6. Eickmeier O, Seki H, Haworth O, Hilberath JN, Gao F, Uddin M, et al. Aspirin-triggered resolvin D1 reduces mucosal inflammation and promotes resolution in a murine model of acute lung injury. Mucosal Immunol. 2012; 6(2):256–266. [PubMed: 22785226]
7. Lozano R, Naghavi M, Foreman K, Lim S, Shibuya K, Aboyans V, et al. Global and regional mortality from 235 causes of death for 20 age groups in 1990 and 2010: a systematic analysis for the Global Burden of Disease Study 2010. Lancet. 2012; 380(9859):2095–2128. [PubMed: 23245604]
8. Peleg AY, Hooper DC. Hospital-acquired infections due to gram-negative bacteria. N Engl J Med. 2010; 19(362):1804–1813.
9. Mizgerd JP. Acute Lower Respiratory Tract Infection. N Engl J Med. 2008; 358(7):716–727. [PubMed: 18272895]
10. Eddens T, Kolls JK. Host defenses against bacterial lower respiratory tract infection. Current opinion in immunology. 2012; 24(4):424–430. [PubMed: 22841348]
11. Serhan CN. Pro-resolving lipid mediators are leads for resolution physiology. Nature. 2014; 510(7503):92–101. [PubMed: 24899309]
12. Palmer CD, Mancuso CJ, Weiss JP, Serhan CN, Guinan EC, Levy O. 17(R)-Resolvin D1 differentially regulates TLR4-mediated responses of primary human macrophages to purified LPS and live E. coli. Journal of leukocyte biology. 2011; 90(3):459–470. [PubMed: 21653234]
13. Duan M, Li WC, Vlahos R, Maxwell MJ, Anderson GP, Hibbs ML. Distinct macrophage subpopulations characterize acute infection and chronic inflammatory lung disease. J Immunol. 2012; 189(2):946–955. [PubMed: 22689883]
14. Herold S, Tabar TS, Janssen H, Hoegner K, Cabanski M, Lewe-Schlosser P, et al. Exudate macrophages attenuate lung injury by the release of IL-1 receptor antagonist in gram-negative pneumonia. Am J Respir Crit Care Med. 2011; 183(10):1380–1390. [PubMed: 21278303]
15. Colas RA, Shinohara M, Dalli J, Chiang N, Serhan CN. Identification and signature profiles for pro-resolving and inflammatory lipid mediators in human tissue. American journal of physiology Cell physiology. 2014; 307(1):C39–54. [PubMed: 24696140]
16. Seki H, Fukunaga K, Arita M, Arai H, Nakanishi H, Taguchi R, et al. The anti-inflammatory and proresolving mediator resolvin E1 protects mice from bacterial pneumonia and acute lung injury. J Immunol. 2009; 184(2):836–843. [PubMed: 20007539]

17. Abdulnour RE, Dalli J, Colby JK, Krishnamoorthy N, Timmons JY, Tan SH, et al. Maresin 1 biosynthesis during platelet-neutrophil interactions is organ-protective. Proceedings of the National Academy of Sciences of the United States of America. 2014; 111(46):16526–16531. [PubMed: 25369934]
18. Aven L, Paez-Cortez J, Achey R, Krishnan R, Ram-Mohan S, Cruikshank WW, et al. An NT4/TrkB-dependent increase in innervation links early-life allergen exposure to persistent airway hyperreactivity. FASEB J. 2014; 28(2):897–907. [PubMed: 24221086]
19. Dalli J, Serhan CN. Specific lipid mediator signatures of human phagocytes: microparticles stimulate macrophage efferocytosis and pro-resolving mediators. Blood. 2012; 120(15):e60–72. [PubMed: 22904297]
20. Fiala M, Liu PT, Espinosa-Jeffrey A, Rosenthal MJ, Bernard G, Ringman JM, et al. Innate immunity and transcription of MGAT-III and Toll-like receptors in Alzheimer's disease patients are improved by bisdemethoxycurcumin. Proc Natl Acad Sci U S A. 2007; 104(31):12849–12854. [PubMed: 17652175]
21. Flo TH, Smith KD, Sato S, Rodriguez DJ, Holmes MA, Strong RK, et al. Lipocalin 2 mediates an innate immune response to bacterial infection by sequestrating iron. Nature. 2004; 432(7019):917–921. [PubMed: 15531878]
22. Kasuga K, Yang R, Porter TF, Agrawal N, Petasis NA, Irimia D, et al. Rapid appearance of resolvin precursors in inflammatory exudates: novel mechanisms in resolution. J Immunol. 2008; 181(12):8677–8687. [PubMed: 19050288]
23. Miki Y, Yamamoto K, Taketomi Y, Sato H, Shimo K, Kobayashi T, et al. Lymphoid tissue phospholipase A2 group IID resolves contact hypersensitivity by driving antiinflammatory lipid mediators. J Exp Med. 2013; 210(6):1217–1234. [PubMed: 23690440]
24. Levy BD, Romano M, Chapman HA, Reilly JJ, Drazen J, Serhan CN. Human alveolar macrophages have 15-lipoxygenase and generate 15(S)-hydroxy-5,8,11-cis-13-trans-eicosatetraenoic acid and lipoxins. J Clin Invest. 1993; 92(3):1572–1579. [PubMed: 8376607]
25. Kim JH, Sherman ME, Curriero FC, Guengerich FP, Strickland PT, Sutter TR. Expression of cytochromes P450 1A1 and 1B1 in human lung from smokers, non-smokers, and ex-smokers. Toxicology and applied pharmacology. 2004; 199(3):210–219. [PubMed: 15364538]
26. Divanovic S, Dalli J, Jorge-Nebert LF, Flick LM, Galvez-Peralta M, Boespflug ND, et al. Contributions of the three CYP1 monooxygenases to pro-inflammatory and inflammation-resolution lipid mediator pathways. J Immunol. 2013; 191(6):3347–3357. [PubMed: 23956430]
27. Levy BD, Serhan CN. Resolution of Acute Inflammation in the Lung. Annu Rev Physiol. 2014; 76:467–92. [PubMed: 24313723]
28. Haworth O, Cernadas M, Yang R, Serhan CN, Levy BD. Resolvin E1 regulates interleukin 23, interferon-gamma and lipoxin A4 to promote the resolution of allergic airway inflammation. Nat Immunol. 2008; 9(8):873–879. [PubMed: 18568027]
29. El Kebir D, Jozsef L, Pan W, Wang L, Petasis NA, Serhan CN, et al. 15-epi-lipoxin A4 inhibits myeloperoxidase signaling and enhances resolution of acute lung injury. Am J Respir Crit Care Med. 2009; 180(4):311–319. [PubMed: 19483113]
30. Hsiao HM, Thatcher TH, Levy EP, Fulton RA, Owens KM, Phipps RP, et al. Resolvin D1 attenuates polyinosinic-polycytidylic acid-induced inflammatory signaling in human airway epithelial cells via TAK1. J Immunol. 2014; 193(10):4980–4987. [PubMed: 25320283]
31. Spite M, Norling LV, Summers L, Yang R, Cooper D, Petasis NA, et al. Resolvin D2 is a potent regulator of leukocytes and controls microbial sepsis. Nature. 2009; 461(7268):1287–1291. [PubMed: 19865173]
32. Gobbetti T, Coldewey SM, Chen J, McArthur S, le Faouder P, Cenac N, et al. Nonredundant protective properties of FPR2/ALX in polymicrobial murine sepsis. Proc Natl Acad Sci U S A. 2014; 111(52):18685–18690. [PubMed: 25512512]
33. Rogerio AP, Haworth O, Croze R, Oh SF, Uddin M, Carlo T, et al. Resolvin D1 and aspirin-triggered resolvin D1 promote resolution of allergic airways responses. J Immunol. 2012; 189(4): 1983–1991. [PubMed: 22802419]

34. Chiang N, Fredman G, Backhed F, Oh SF, Vickery T, Schmidt BA, et al. Infection regulates pro-resolving mediators that lower antibiotic requirements. Nature. 2012; 484(7395):524–528. [PubMed: 22538616]

35. Bystrom J, Evans I, Newson J, Stables M, Toor I, van Rooijen N, et al. Resolution-phase macrophages possess a unique inflammatory phenotype that is controlled by cAMP. Blood. 2008; 112(10):4117–4127. [PubMed: 18779392]

36. Schif-Zuck S, Gross N, Assi S, Rostoker R, Serhan CN, Ariel A. Saturated-efferocytosis generates pro-resolving CD11b low macrophages: modulation by resolvins and glucocorticoids. European journal of immunology. 2011; 41(2):366–379. [PubMed: 21268007]

37. Poe SL, Arora M, Oriss TB, Yarlagadda M, Isse K, Khare A, et al. STAT1-regulated lung MDSC-like cells produce IL-10 and efferocytose apoptotic neutrophils with relevance in resolution of bacterial pneumonia. Mucosal Immunol. 2013; 6(1):189–199. [PubMed: 22785228]

38. Organization, WH. Antimicrobial resistance: global report on surveillance 2014. World Health Organization; Apr. 2014 2014

39. Meijvis SCA, Hardeman H, Remmelts HHF, Heijligenberg R, Rijkers GT, van Velzen-Blad H, et al. Dexamethasone and length of hospital stay in patients with community-acquired pneumonia: a randomised, double-blind, placebo-controlled trial. Lancet. 2011; 377(9782):2023–2030. [PubMed: 21636122]

40. Van Den Berg C, de Neeling AJ, Schot CS, Hustinx WN, Wemer J, de Wildt DJ. Delayed antibiotic-induced lysis of Escherichia coli in vitro is correlated with enhancement of LPS release. Scandinavian journal of infectious diseases. 1992; 24(5):619–627. [PubMed: 1465580]

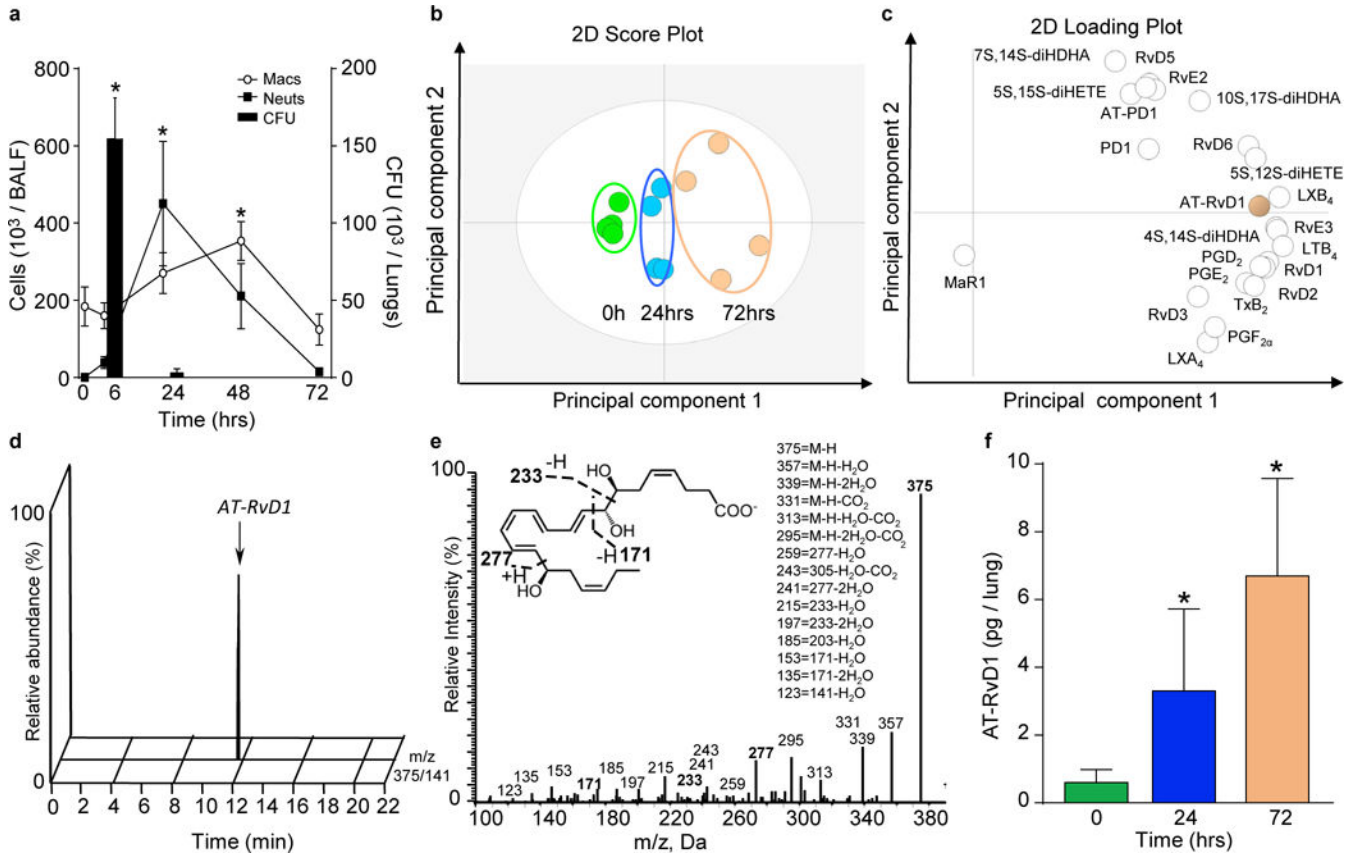

Figure 1. Endogenous AT-RvD1 is produced during bacterial pneumonia

(a) Time course of murine lung CFU, and BAL neutrophils and macrophages, at indicated time points after infection (*E. coli*, 10^6 CFU, IB). Results expressed as mean ± SD, n > 5 mice in two independent experiments, * P < 0.05 vs 0 and 72 hrs. (b–f) Lipids were extracted from murine lungs 0, 24, and 72 hrs after infection and LM-SPM profiles were obtained using LC-MS/MS metabololipidomics as in Methods. (b) Two-dimensional score plot and (c) loading plot of a principal component analysis of murine LM-SPM signature profiles. The white ellipse in the score plot denotes 95% confidence regions. (d) Representative multiple reaction monitoring (MRM) chromatogram (m/z = 375>141) and (e) MS/MS spectrum, obtained from infected murine lung, used for the identification of AT-RvD1 (7*S*,8*R*,17*R*-trihydroxy-docosa-4Z,9E,11E,13Z,15E,19Z-hexaenoic acid). (f) AT-RvD1 levels in murine lungs during pneumonia (n = 4 per time point, mean ± SD, * P < 0.05 vs 0 hrs).

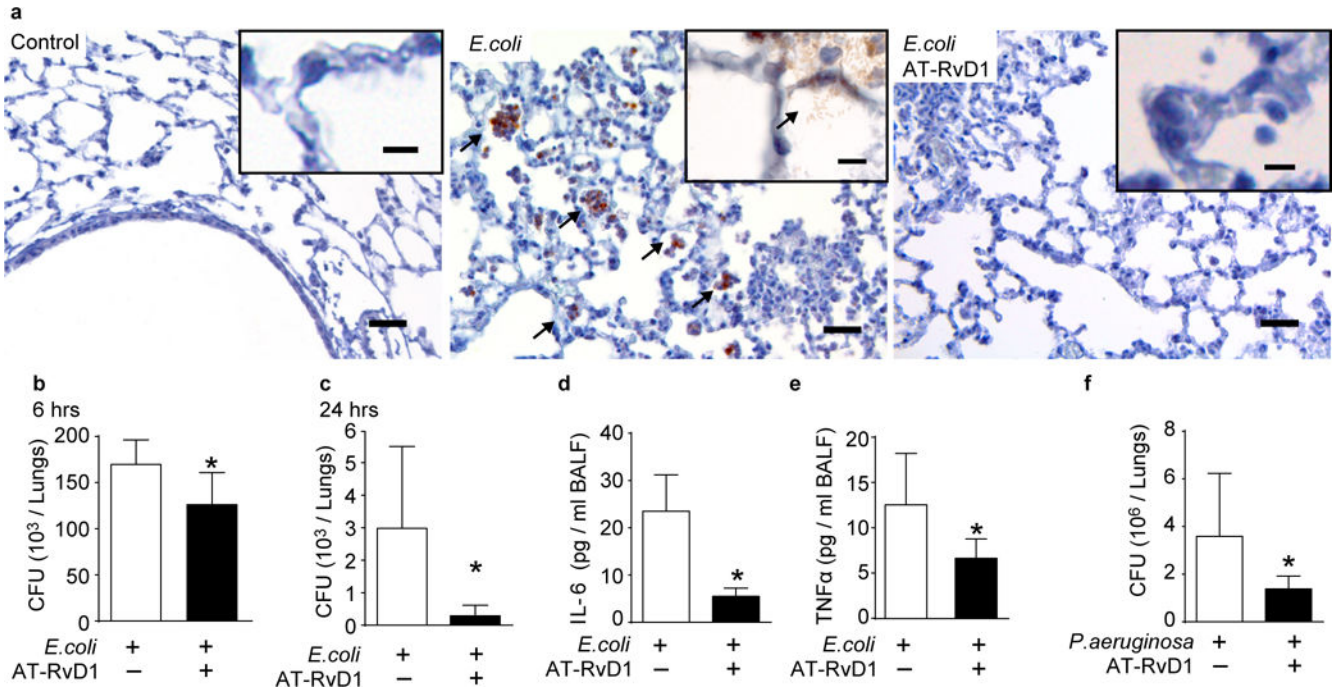

Figure 2. AT-RvD1 enhances bacterial clearance

(a) Representative lung sections from control mice, and 24 hrs after infection and treatment with AT-RvD1 or vehicle stained with an anti-*E. coli* antibody. Arrowheads indicate *E. coli*, bar = 50 μm, inset bar = 10 μm. Lung *E. coli* CFU counts (b) 6 hrs and (c) 24 hrs after infection (10^6 CFU, IB) in mice treated with AT-RvD1 or vehicle. Levels of (d) IL-6 and (e) TNF-α 6 hrs after infection determined by bead-based immunoassay. (f) Lung *P. aeruginosa* CFU counts 6 hrs after infection (10^6 CFU, IB) in mice treated with AT-RvD1 or vehicle. In all experiments, AT-RvD1 (100 ng, IV) or vehicle (< 0.1% EtOH in saline vol/vo, IV) were given 1 hr after *E. coli*. Results are expressed as mean ± SD n = 4–7 per group. * $P < 0.05$

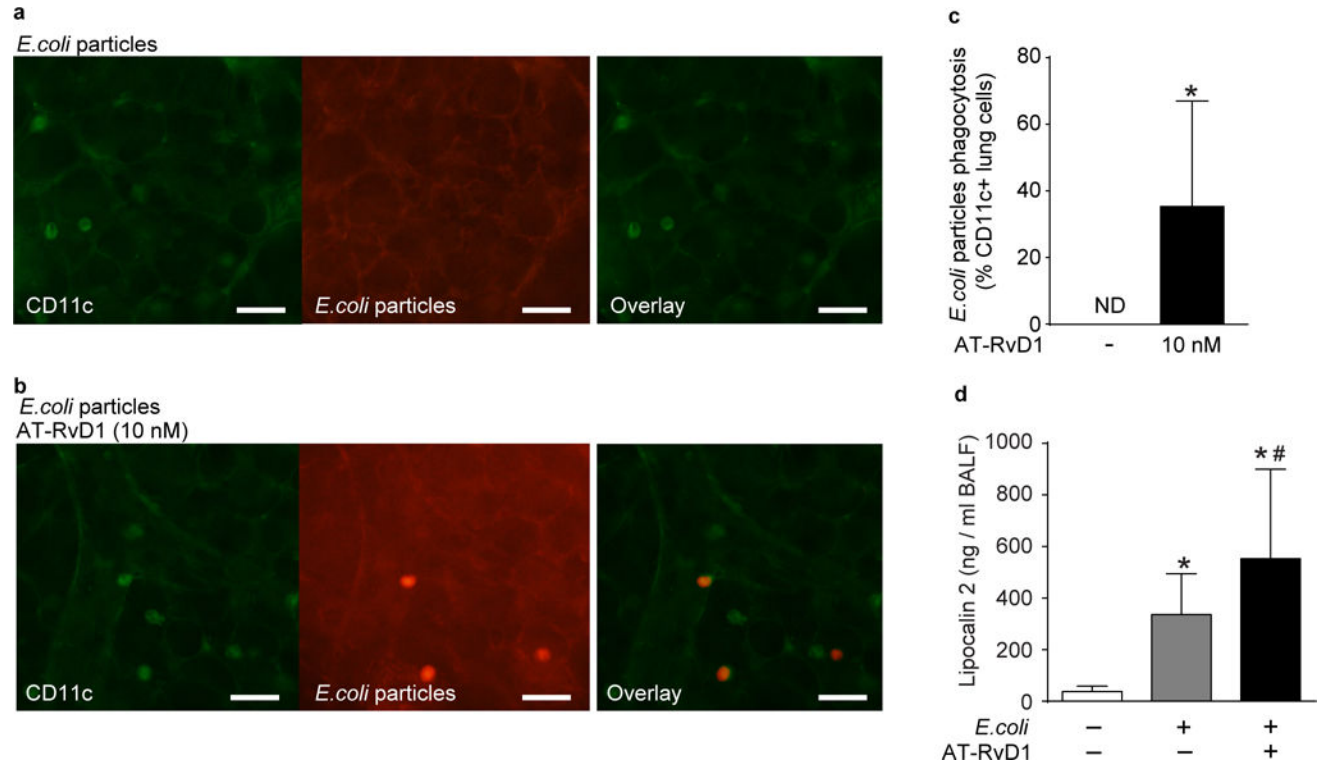

Figure 3. AT-RvD1 increases bacterial phagocytosis by CD11c$^+$ lung cells

Ultra-thin perfused lung sections were obtained from naïve mice, stained with anti-CD11c, and treated with AT-RvD1 (10 nM, 45 minutes, 37°C) or vehicle. Sections were then co-incubated with *E. coli* particles labelled with a pH-sensitive probe (100 μg/ml, 60 minutes, RT) and imaged using a fluorescence microscope. Particle dose was chosen to give minimal phagocytosis in vehicle treated sections. Representative images of (a) control and (b) AT-RvD1 treated lung sections. (c) Proportion of CD11c+ lung cells participating in phagocytosis of *E. coli* particles. * $P < 0.05$. (d) Lipocalin 2 levels in BAL fluid 6 hrs after *E. coli* infection determined by ELISA. Results are expressed as mean ± SD $n = > 8$ sections per group in two independent experiments. * $P < 0.05$ vs vehicle treated un-infected mice, # $P < 0.05$ vs vehicle treated infected mice.

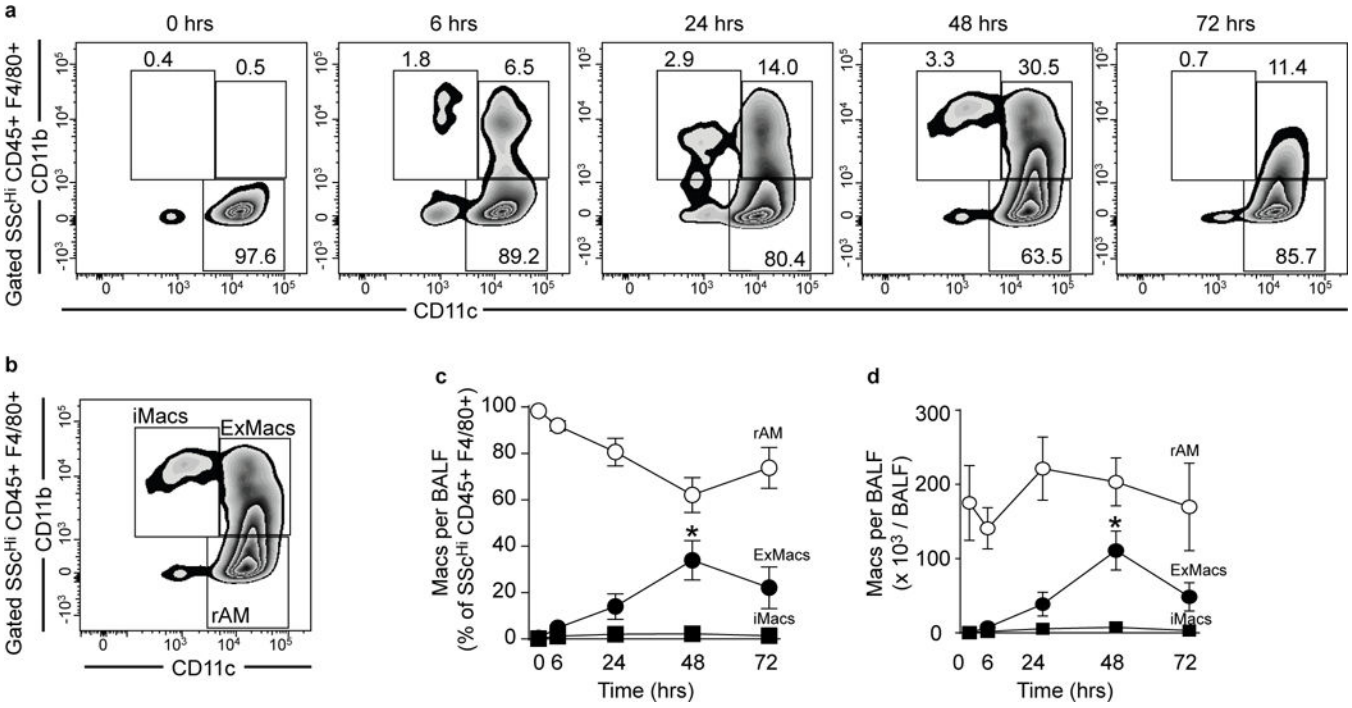

Figure 4. Macrophage subsets during *E. coli* pneumonia

BAL was obtained from mice at determined time-points after *E. coli* infection (10^6 CFU, IB) for macrophage subset enumeration by flow cytometry. (a) Representative flow cytometry dot plots from BAL gated on macrophages (SSc^{Hi} $CD45^+$ $F4/80^+$). (b) Identification of macrophage subsets based on CD11b and CD11c surface expression as infiltrating (iMacs, $CD11c^{Low}$ $CD11b^{Hi}$), exudative (ExMacs, $CD11c^{Hi}$ $CD11b^{Hi}$), and resident Alveolar Macrophages (rAM, $CD11c^{Hi}$ $CD11b^{-}$). Time course of BAL macrophage subset (c) fractions and (d) counts. Results are expressed as mean ± SD. $n = 10$ mice per group from 2 independent experiments, * $P < 0.05$

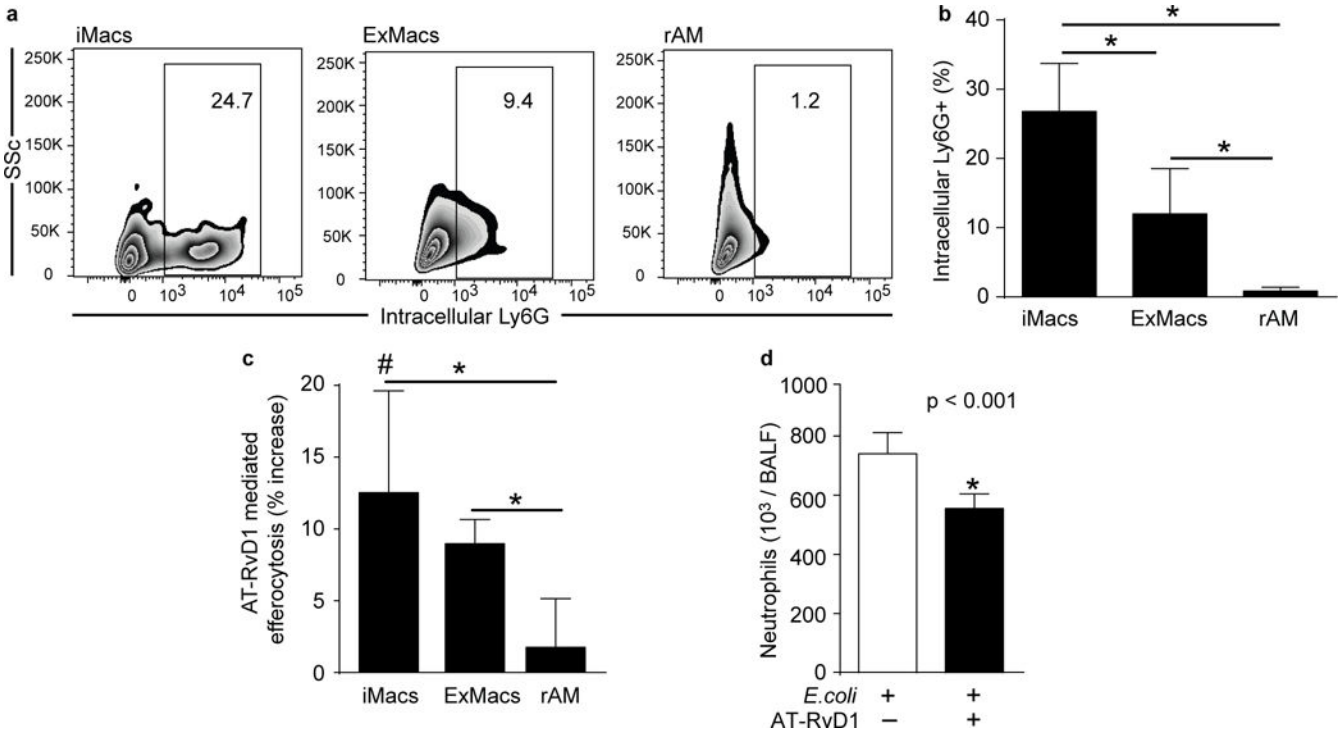

Figure 5. Recruited macrophages participate in efferocytosis of neutrophils during resolution of pathogen-mediated inflammation

(a) Representative dot plots and (b) bar-graph of intracellular Ly6G staining gated on macrophage subsets in BAL obtained 48 hrs after infection. Results are expressed as mean ± SD. n = 4 sections per group in two independent experiments. (c) Percent increase in efferocytosis of apoptotic neutrophils by macrophage subsets after treatment with AT-RvD1 compared to vehicle (10nM, 30 min, 37°C). Macrophage and apoptotic neutrophil preparations are detailed in Methods. Results are expressed as mean ± SD. n = > 10 per group. ♯ P < 0.05 vs vehicle treated (d) Neutrophil count in BAL obtained from mice 48 hrs after high-dose infection (*E. coli*, 2×10^6 CFU, IB) and treatment with AT-RvD1 (100ng, IB) 24 and 36 hrs after *E. coli*. Results are expressed as mean ± SD. n = 10 mice per group from 2 independent experiments. In all figures, * P < 0.05

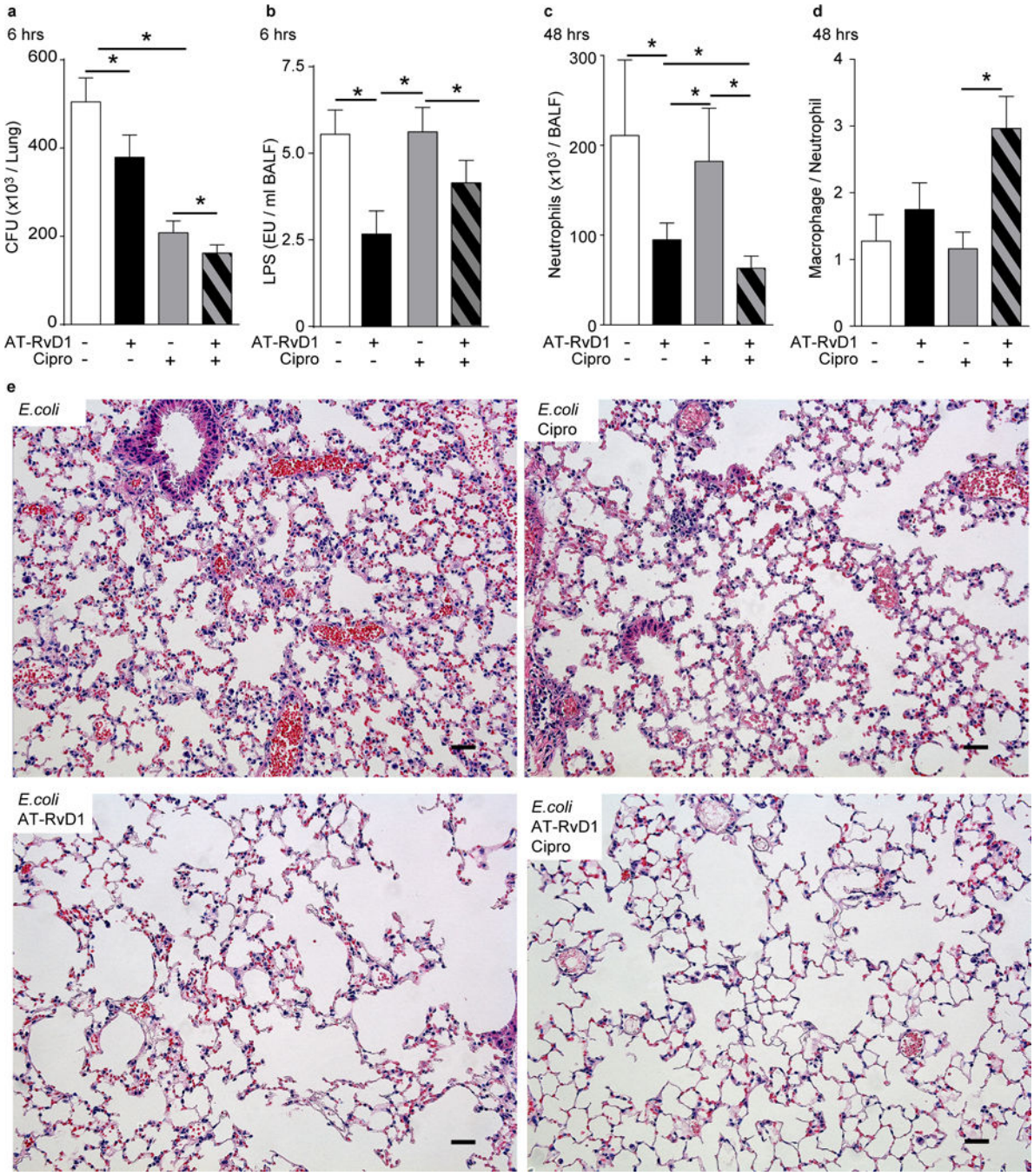

Figure 6. AT-RvD1 enhances bacterial clearance in combination with antibiotics

(a) Lung CFU counts and (b) BAL fluid LPS concentrations (Endotoxin Units/ml BAL fluid) 6 hrs after *E. coli* infection, and (c) BALF neutrophils and (d) BALF macrophage to neutrophil ratio (a resolution index) 48 hrs after infection with *E. coli* (10^6 CFU, IB) in mice treated with AT-RvD1 (100 ng, IV, 1 hr after infection) or vehicle (< 0.1% EtOH in saline vol/vol), with or without ciprofloxacin (0.2 mg/kg, IP, 1 hr after infection). Results are

expressed as mean ± SD. n = 5–7 per group. * P < 0.05 (e) Representative hematoxylin and eosin stains of murine lungs 48 hrs after infection. n = 3 per group.

Mucosal Immunol. Author manuscript; available in PMC 2016 November 14.

Table 1

Mouse lung lipid mediators (pg/lung)

	Q1	Q3		0 hrs	SEM		24 hrs	SEM		72 hrs	SEM
RvD1	375	141	**0.4**	±	0.1	**1.6**	±	0.4	**5.1**	±	1.6
RvD2	375	175	**0.8**	±	0.3	**10.7**	±	3.7	**36.4**	±	12
RvD3	375	147	**0.2**	±	0.1	**1.2**	±	0.5	**2.7**	±	1
RvD5	359	199	**16.2**	±	7.8	**14.8**	±	6.8	**35.2**	±	4.5
RvD6	359	159	**2.4**	±	0.3	**2.7**	±	0.4	**6.8**	±	1.1
AT-RvD1	375	141	**0.6**	±	0.2	**3.3**	±	1.1	**6.7**	±	1.4
AT-RvD3	375	147	*		*	*		*	*		*
PD1	359	153	**0.7**	±	0.1	**2.5**	±	0.7	**3.8**	±	0.8
10S,17S-diHDHA	359	153	**41.7**	±	23.6	**209.9**	±	119.2	**394.1**	±	58.5
AT-PD1	359	153	**0.8**	±	0.2	**4.2**	±	1	**8.7**	±	4.5
MaR1	359	177	**0.7**	±	0.3	*	±	*	*	±	*
RvE1	349	161	*	±	*	*	±	*	*	±	*
RvE2	333	253	**4.5**	±	0.6	**4.9**	±	1.6	**42.7**	±	20.1
RvE3	333	201	**5.4**	±	1.3	**66**	±	22	**199.3**	±	48.2
LxA4	351	115	**4.5**	±	1.9	**49.2**	±	24	**102.4**	±	54.1
LxB4	351	221	**123.5**	±	0.6	**696.6**	±	1.6	**1094**	±	20.1

* = below limit (0.1pg)